altitudes were studied: 125,000 ft with a drag D_f of 119 lbf, and 200,000 ft with a drag of 17.4 lbf.

For the exponential profile, B and V were taken to be 0.271, which at the base radius reduces the species values to one percent of their centerline value. For the parabolic, B and V were taken as 1.23, reducing the species to zero at the base radius.

Figure 1 describes the ionization for the various profile shapes. As would be expected, the exponential profile with its sharp peak at the centerline is most reduced by diffusion. The parabolic profile, which might be considered more realistic, shows small reduction due to diffusion at an altitude of 125,000 ft.

Figure 2 describes the ionization predicted for a parabolic profile at 200,000 ft. It is seen that diffusion has a stronger effect at this altitude for the same x, although the stream-tube prediction is still well within an order of magnitude. The fact that diffusion has a larger effect at lower Reynolds numbers could be predicted from Eq. (23) as well as physically

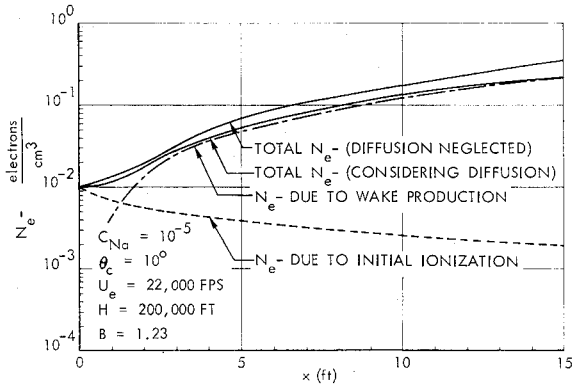

Fig. 2 Sodium ionization at 200,000 ft for parabolic profiles.

anticipated. Figures 1 and 2 describe the breakdown of the ionization into its two components: that due to initial ionization and that due to wake production.

Conclusions

1) The effects of diffusion in laminar hypersonic wakes depend on altitude and specie profile shapes. For parabolic shapes (perhaps physically more reasonable) and for the conditions considered, diffusion has small effect on the centerline electron densities.

2) In contrast to the boundary layer, wake solutions neglecting diffusion [stream-tube or Eq. (21)] are then useful in providing reasonably accurate predictions of contaminated laminar wake ionization if one assumes parabolic radial variations in specie profiles and ion production.

References

[1] Kane, J. J., "Nonequilibrium sodium ionization in laminar boundary layers," AIAA J. 2, 1651–1653 (1964).

[2] Fernandez, F. L. and Levinsky, E. S., "Air ionization in the hypersonic laminar wake of sharp cones," Aerospace Corp., Rept. TDR-269 (S5811-20)-1 (June 1964).

[3] Pallone, A. J., Erdos, J. I., Eckerman, J., and McKay, W., "Hypersonic laminar wakes and transition studies," AIAA Preprint 63-171 (June 1963).

[4] Bortner, M. H., "Chemical kinetics in a re-entry flow field," Space Sciences Lab., General Electric Missile and Space Div., R63SD63 (August 1963).

[5] Levinsky, E. S. and Fernandez, F. L., "Approximate nonequilibrium air ionization in hypersonic flows over sharp cones," Aerospace Corp., Rept. TDR-269 (S4810-60)-1 (November 1963).

Electrical Properties of Rocket Nozzle Boundary Layers

LEROY J. KRZYCKI*
U. S. Naval Ordnance Test Station, China Lake, Calif.

RECENT engineering applications of plasma physics have uncovered several previously unsuspected areas of practical difficulty. This note treats one of these areas, namely, the low level of ionization existing in the boundary layer of partially-ionized gas flows. Magnetogasdynamic (MGD) electrical power generators,[1] MGD accelerators,[2] and magnetotransport experiments[3] have all encountered electrical conductivity problems that can be directly associated with the boundary layer separating the electrode or wall from the core flow. The boundary layer acts like a poor electrical insulator, effectively isolating the partially-ionized core flow from the containment walls.[4]

In support of the experiment discussed in Ref. 3, calculations were undertaken which defined, in the absence of an applied magnetic field, the gas electrical properties in the core and boundary layer of a contoured rocket nozzle. The products of a gaseous oxygen-methyl alcohol combustion process flowed through the nozzle as shown in Fig. 1. The reactants were seeded with cesium carbonate to increase the free electron number density and electrical conductivity of the combustion products.

Calculations

The analysis began with the calculation of the thermodynamic properties of the combustion product gas flowing into the nozzle. Pressure and thermochemical parameters associated with an actual experiment[3] were used as the basis for these calculations. A chemical-equilibrium digital computer program[5] was used to determine the gas temperature, chemical species, other thermodynamic properties, and the free electron number density of the gases in the combustion chamber and the nozzle core flow. The IBM 7094 chemical-equilibrium program considered ionic as well as chemical reactions; the expansion process was based on shifting equilibrium and dissociation of the combustion products. For a combustion pressure of 4.28 atm and an oxidizer-fuel ratio of 1.32 with a seed rate of 4.4% of total flow (by weight), the calculations indicated the stagnation combustion temperature to be 3004°K. On the nozzle core centerline, the static temperature at the geometric sonic throat was calculated at 2873°K, the ratio of specific heats was 1.196, the electron density was 1.39×10^{15} e^-/cm^3, and 0.0269 g-moles of monatomic cesium gas per 100 g of constituents were available for thermal ionization.

The heat transfer through and thickness of the boundary layer on the hot-gas side of the rocket nozzle were calculated using a programed differential equation method, described in Ref. 6. The IBM 7094 program, obtained from Jet Propulsion Laboratory (JPL) and modified by Navel Ordnance Test Station (NOTS), calculated the following as functions of

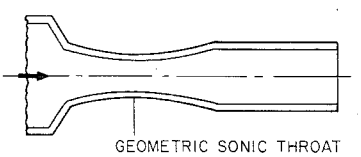

Fig. 1 Contoured convergent-divergent nozzle. Throat diameter is 0.0127 m. Boundary-layer gas-electrical properties discussed in this note were calculated at the geometric sonic throat.

Received October 5, 1964.

* Research Aerospace Engineer, Advanced Technology Division, Propulsion Development Department. Member AIAA.

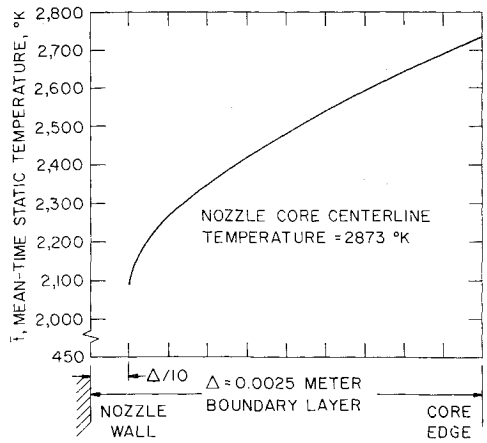

Fig. 2 Boundary-layer static gas temperature at the geometric sonic throat as a function of distance from the nozzle wall. Nozzle throat static pressure (2.44 atm) is constant across the boundary layer to the nozzle wall. There is no applied magnetic field.

axial position within the nozzle: velocity, temperature, displacement, momentum, and energy boundary-layer thicknesses; hot-gas film heat-transfer coefficient; heat flux to the nozzle wall; cumulative heat transfer to the wall, and the skin-friction coefficient. The program also printed out the Mach number and static temperature in the core flow at the edge of the boundary layer. The method solved, simultaneously, the integral momentum and energy equations for thin axisymmetric boundary layers. Boundary-layer shape parameters were approximated from one-seventh-power profiles of velocity and stagnation temperature, and skin-friction coefficient and Stanton number were evaluated as functions of boundary-layer thickness from the best available semiempirical relations. The digital computer program was modified from the basic JPL program to calculate and print out the mean-time static temperature in the constant pressure boundary layer as a function of distance from the nozzle wall. The results of the static temperature calculation at the geometric sonic throat of the nozzle are shown in Fig. 2. Numerous calculations were made both upstream and downstream of the sonic location; the data shown are typical of those calculations. Based on thermocouple data, the wall temperature for the calculations was assumed constant over the nozzle region at 450°K. As shown in Fig. 2, the static temperature decreases almost linearly to the approximate interface between the laminar sublayer and the buffer region. In the laminar sublayer, the temperature gradient is quite steep.

A modified version of the chemical-equilibrium program mentioned previously[5] was used to compute, as a function of distance from the nozzle wall, the amounts of the numerous chemical species present in the boundary layer. A homogeneous gas mixture with a composition similar to that burned in the combustion chamber was assumed to exist in the boundary layer. As inputs, this modified program required gas pressure, temperature, and stoichiometry conditions.

The electrical properties of the nozzle core and boundary-layer gas were then calculated as a function of distance from the nozzle wall by an electrical conductivity program.[1] This program calculated the degree of thermal ionization of monatomic cesium gas from a modified Saha equation and the electrical conductivity and free electron number density in terms of the thermodynamic variables of the seeded gas. The electrons were assumed to be produced solely by thermal ionization of seed gas atoms, an assumption previously substantiated by results from the chemical-equilibrium program, which employed ionic equations and considered both electron formation and attachment,[5] and by microwave attenuation measurements on the free exhaust of a rocket engine burning a

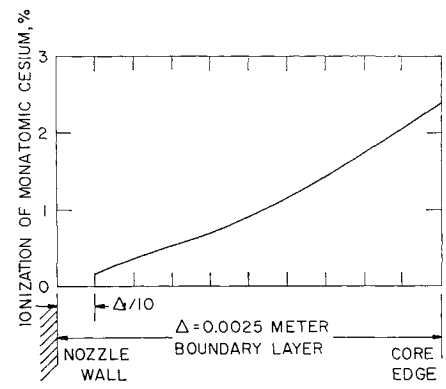

Fig. 3 Percentage ionization of monoatomic cesium gas as a function of boundary-layer thickness.

similar, seeded, hydrocarbon propellant combination.[7] The results of these calculations are shown in Figs. 3 and 4. Figure 3 indicates the percentage ionization of the monatomic cesium gas in the boundary layer, and Fig. 4 indicates the decrease in gas-electrical properties associated with the decrease in gas-static temperature in the nozzle boundary layer. The boundary layer effectively shields the core flow from the nozzle wall.

Conclusion

Using several digital computer programs, the electrical properties of a rocket-nozzle boundary layer were calculated. There was no applied magnetic field. Calculations were performed for an actual experimental device. The gas-electrical conductivity and electron density decreased by a factor of 10 in the boundary layer and decreased even more rapidly in the laminar sublayer. The calculation procedures described are applicable to a wide variety of magnetofluid engineering devices. The low boundary-layer ionization indicated by this study partially explains the poor performance of many recent magnetofluids devices.

Unless a method is found for ionizing the boundary layer (perhaps by fabricating the wall from a porous material and employing surface ionization of alkali-metal vapor forced through the porous material), the success of magnetofluid devices employing flowing, thermally ionized gases will be limited.

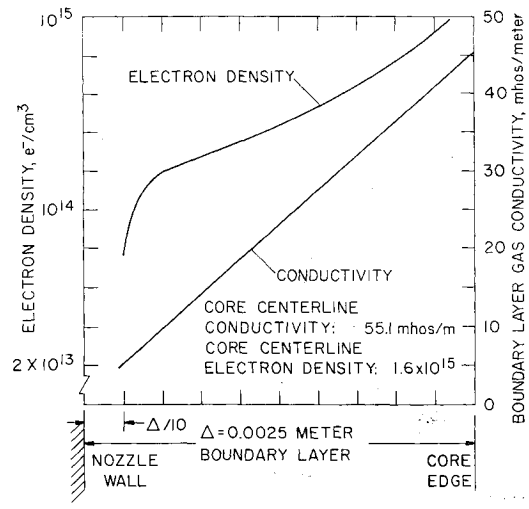

Fig. 4 Boundary-layer gas-electrical conductivity and electron density at the geometric sonic throat of the nozzle as a function of distance from the nozzle wall. There is no applied magnetic field. Nozzle throat static pressure (2.44 atm) is constant across the boundary layer to the nozzle wall.

References

[1] Krzycki, L. J., Larsen, H. M., and Byrne, W. M., Jr., "Magneto-hydrodynamic power generation from a supersonic rocket exhaust," U. S. Naval Ordnance Test Station, China Lake, Calif., NOTS TP 3186, Bureau of Naval Weapons NAVWEPS Rept. 8111 (December 1962).

[2] Blackman, V. H. and Sunderland, R. J., "Experimental performance of a crossed-field plasma accelerator," AIAA J. 1, 2047 (1963).

[3] Krzycki, L. J. and Lee, J. B., "The effect of an intense magnetic field on rocket nozzle heat transfer, part II: cryogenic electromagnet experiments," U. S. Naval Ordnance Test Station, China Lake, Calif., NOTS TP 3545, Bureau of Naval Weapons NAVWEPS Rept. 8494 (June 1964).

[4] Hale, F. J. and Kerrbrock, J. L., "Insulator boundary layers in magnetohydrodynamic channels," AIAA J. 2, 461 (1964).

[5] Browne, H. N., Williams, M. M., and Cruise, D. R., "The theoretical computation of equilibrium compositions, thermodynamic properties and performance characteristics of propellant systems," U. S. Naval Ordnance Test Station, China Lake, Calif., NOTS TP 2434, Bureau of Naval Weapons NAVWEPS Rept. 7043 (June 1960).

[6] Elliott, D. G., Bartz, D. R., and Silver, S., "Calculation of turbulent boundary-layer growth and heat transfer in axisymmetric nozzles," Jet Propulsion Lab., California Institute of Technology, Pasadena, Calif., TR 32-387 (February 1963).

[7] Larsen, H. M. and Turner, C. H., "Microwave measurement of electron density in seeded rocket exhaust gases," U. S. Naval Ordnance Test Station, China Lake, Calif., NOTS TP 3062, Bureau of Naval Weapons NAVWEPS Rept. 8059 (June 1963).

Buckling of a Cylindrical Shell Loaded by a Pre-Tensioned Filament Winding

MARTIN M. MIKULAS JR.* AND MANUEL STEIN†
NASA Langley Research Center, Hampton, Va.

Nomenclature

D	=	plate flexural stiffness, $Et^3/12(1-\mu^2)$
E	=	Young's modulus
k	=	elastic spring constant
k_y	=	buckling coefficient, $NL^2/D\pi^2$
K	=	spring stiffness parameter, $kL^4/\pi^4 D$
L	=	length of cylinder
n	=	number of waves in circumferential direction
N	=	applied circumferential stress resultant
N_x, N_y, N_{xy}	=	in-plane stress resultants
r	=	radius of cylindrical shell
t	=	thickness of cylindrical shell
u,v,w	=	displacements in the x-, y-, and radial directions, respectively
x,y	=	axial and circumferential coordinates, respectively
Z	=	curvature parameter, $(L^2/rt)(1-\mu^2)^{1/2}$
$\epsilon_x, \epsilon_y, \gamma_{xy}$	=	in-plane strains
μ	=	Poisson's ratio
∇^4	=	$\partial^4/\partial x^4 + 2(\partial^4/\partial x^2\partial y^2) + \partial^4/\partial y^4$
∇^{-4}	=	inverse operator defined by equation $\nabla^{-4}(\nabla^4 f) = \nabla^4(\nabla^{-4} f) = f$
0	=	subscript referring to filament winding

When the subscripts x and y follow a comma, they indicate partial differentiation with respect to x and y, respectively.

Introduction

DESIGNS have appeared recently in launch-vehicle technology in which circular-cylindrical shells are wrapped with pre-tensioned filaments. An example of such a design is a cylinder that is wrapped circumferentially to help carry hoop stress from internal pressure. Another example is a cylindrical cryogenic tank upon which insulation is held in place by pre-tensioned filaments to protect against aerodynamic heating. One question that arises in the design of such configurations is: What is the largest filament tension that can be allowed before buckling of the shell would occur? It is believed that the theoretical analysis presented in this note is a contribution toward answering this question.

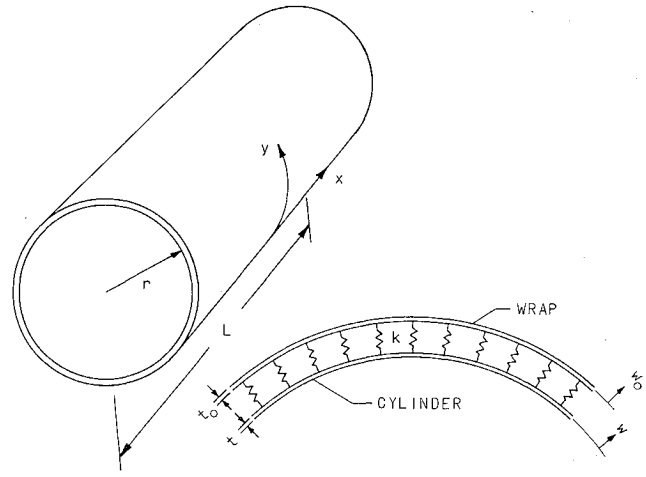

Fig. 1 Configuration and coordinate system.

An idealized model of the configuration is studied in which material compressibility in the thickness direction is represented by many closely spaced, independent, radial springs located between the shell and the filaments. For the case of insulation secured to the shell by filament winding, the springs represent essentially the thickness compressibility of the insulation. For the case of filaments wrapped directly on the shell, the springs represent some effective thickness compressibility of the shell and filaments. A simple, closed-form solution is obtained for the idealized model. Results are plotted in dimensionless form so that the buckling load (the critical tension in the filaments or the critical compression in the shell) can be obtained directly for wide ranges of the geometrical and stiffness parameters of the model.

Analysis

The buckling of an elastic isotropic, homogeneous, circular-cylindrical shell loaded through many closely spaced, radial springs by pre-tensioned circumferentially wrapped filaments is analyzed (see Fig. 1). The filament winding is considered to have no bending stiffness. The difference between the radius of the shell and of the filaments is assumed to be negligible so that the hoop tension per unit length in the filaments N causes an equal magnitude of hoop compression $-N$ in the shell. The filaments are permitted to slide freely relative to the cylinder and relative to each other; i.e., no bonding agent is applied to the filaments or the cylinder. Thus the hoop tension load per unit length in the filament winding is simply the number of filaments per unit length times the load in each filament.

For changes in stress resultants and displacements, which occur during buckling, the equilibrium equations are, for the shell,

$$N_{x,x} + N_{xy,y} = 0 \tag{1}$$

$$N_{y,y} + N_{xy,x} = 0 \tag{2}$$

$$D\nabla^4 w + (N_y/r) + Nw_{,yy} + k(w - w_0) = 0 \tag{3}$$

and, for the filament winding,

$$N_{y0,y} = 0 \tag{4}$$

Received September 29, 1964.

* Aerospace Engineer.

† Aerospace Engineer. Associate Fellow Member AIAA.